

Chapter 2

Growth Model

In this chapter, we present our growth model for ultrathin films. While other studies of magnetic film systems usually apply very simplified growth modes, like treating islands as ideal geometrical objects or assuming purely random adatom deposition, more realistic morphologies during film growth, ranging from isolated islands to closed layers, shall be considered here. However, to perform calculations for large unit cells and time scales, in addition, the growth model has to be efficient. We apply an extended Eden model of island growth whose main idea is to attach adatoms to already existing islands. The usage of this simple model should be regarded as a first approximation towards a more physically founded description of growing magnetic films.

In **Sec. 2.1**, the extended Eden model is presented. The application of the model to a fast MC simulation of a growing fcc(001) ultrathin film is shown in Appendix B. In **Sec. 2.2**, we present resulting nanostructures. In particular, a bilayer island-type growth mode and its percolation behavior is discussed which serves as a model system for the magnetic calculations of this study.

2.1 Extended Eden model of island growth

Thin films, grown on substrates by molecular beam epitaxy (MBE), where the pseudomorphical formation of the solid phase from the gaseous phase is realized, have been studied for a few decades, but still a detailed description of the time evolution of such systems is a complicated challenge. In Appendix A, we introduce some basic concepts and methods for the theoretical investigation of ultrathin film growth and discuss briefly their advantages and limitations. Only in few cases, equilibrium theories, based on the minimization of the free energy of a growing system, can explain the experimentally observed growth modes [168]. This is due to the fact that film growth evolves via kinetic atomic processes, which often lead to metastable film morpholo-

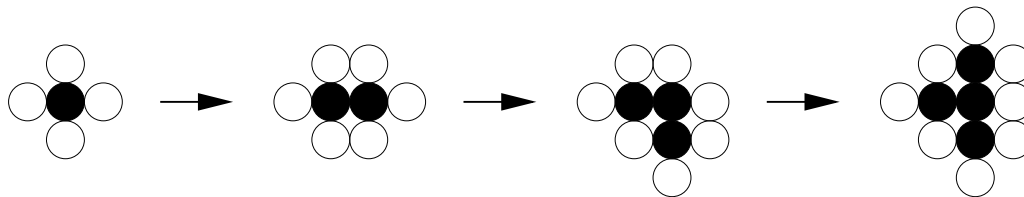


Figure 2.1: Three growth steps of an Eden cluster on a square lattice. Occupied sites are represented by \bullet , perimeter sites by \circ .

gies far from equilibrium. The most important methods which take into account atomic growth processes, are (i) kinetic rate equations [168], and two numerical methods, namely (ii) molecular dynamics [98], and (iii) kinetic Monte Carlo simulations [94]. In particular the latter approach is often the method of choice for the theoretical study of growing thin films [125].

Due to the fact that the present thesis concentrates on the investigation of magnetic properties, we apply an extension of the simple Eden model of growth [43] to the magnetic calculations. On one hand, this model does not require high numerical effort, allowing for the simulation of large systems and coverage ranges. On the other hand, it results in realistic film morphologies.

The original Eden model of a growing cluster on a lattice follows simple geometrical growth rules which are visualized in Fig. 2.1:

- (1) Start from a single occupied lattice site (\bullet), serving as a seed.
- (2) In each growth step occupy an empty perimeter site (\circ), next neighbored to an occupied site (\bullet).

This growth procedure results in clusters with compact structures and was designed by Eden as a simple model for biological systems, e. g. for cancer growth.¹

In the context of thin film growth, this model mimics the attachment of adatoms to already existing islands. The assumption of growing compact islands takes into account that for coverages $\Theta < 1$ ML (monolayer) ultrathin films usually grow in an *island*-type fashion in a wide temperature range, even in case of a layer-by-layer growth mode. This is due to the fact that for sufficiently high temperatures the adatom mobility on the substrate is high

¹The nontrivial aspect of this model is the irregularity of the surface of the Eden clusters which was investigated by several groups [130, 82, 178]. There are at least two different versions of the Eden model in literature. In the first version, in each growth step, all *perimeter sites* have the same probability to be occupied, resulting in a cluster surface which is comparatively rough, but still more compact than for dendritic growth. In the second version all *open bonds* are occupied with equal probability. This growth rule produces somewhat smoother surfaces than the first one.

enough to nucleate islands. As an example, see Fig. 1.1 (a), p. 15, which shows results obtained by STM measurements on the Co/Cu(001) system.² Thus, the Eden model considers implicitly the atomic growth processes (a), (b), (c), and (d) of Fig. A.2, p. 112.

At room temperature, often equilibrated island shapes with edges of low formation energy are observed. For example, in Fig. 1.1 (a) rectangular islands with preferential orientation of the island edges along the $[110]$ and $[\bar{1}\bar{1}0]$ directions can be seen. The reason for the occurrence of equilibrated island shapes is that at sufficiently high temperatures adatoms can diffuse along the island edge 'probing' the perimeter sites with different binding energies, see process (f) in Fig. A.2, p. 112. Hence, even though growth is a kinetic process resulting in metastable morphologies, *local* equilibrium at the island edges can be obtained.³

To consider this, we extend the simple Eden model and occupy a perimeter site with probability p , dependent on the adatom binding energy E^{ad} of the site. For this probability, we apply the Boltzmann factor

$$p \propto \exp(-E^{\text{ad}}/k_{\text{B}} T_{\text{g}}) \quad , \quad (2.1)$$

where T_{g} is the temperature during growth.

Within a 'bond-cutting' model, the adatom binding energy E^{ad} depends on the local coordination number q of the perimeter site. Detailed density functional theory calculations have shown that for metals the dependence of E^{ad} on q can be approximated by [105, 140]

$$E^{\text{ad}} \propto \sqrt{q} \quad . \quad (2.2)$$

This simple formula takes into account that due to quantum mechanics the bond strength saturates at a certain number of neighbors.⁴

To simulate systems up to coverages of several monolayers we allow also for the occupation of perimeter sites in additional layers on top of the interface layer. We apply the so-called solid-on-solid approximation, where the formation of vacancies and overhangs is avoided. By assuming layer dependent *effective* binding parameters A_z we put

$$E^{\text{ad}}(q, z) = -A_z \sqrt{q} \quad , \quad A_z > 0 \quad , \quad (2.3)$$

where $z = 1, \dots, n$ is the layer index. As we will see, using this approach

²It was shown by Pentcheva in an *ab-initio* calculation of the corresponding energy barrier ΔE that diffusion of Co adatoms on a flat Cu(001) terrace is activated for temperatures $T > 231$ K [125].

³Pentcheva calculated in her study of the Co/Cu(001) system that diffusion of Co adatoms along $[110]$ edges is activated for $T > 208$ K [125].

⁴Pentcheva verified this square-root dependence for the Co/Cu(001) system [125].

we are able to simulate with simple means different experimentally observed growth modes, such as 3D-island or layer-by-layer growth mode.⁵

In summary, we use an extended Eden model for the description of island-type growing thin films. The dependence of the occupation probability p , given by Eq. (2.1), on the coordination number q of the perimeter sites determines the island shapes, the dependence on the parameter $A(z)$ results in the growth mode. Different island densities and arrangements can be adjusted to experimental observations by corresponding initial distributions of seeds for the Eden islands according to growth rule (1). The deposition rate of the growing thin film is adjusted by the number of iterations of growth rule (2) in a certain time step Δt .

Clearly, this model can be applied to surfaces of different types. The realization of a MC simulation of the extended Eden model on a fcc-(001) surface is shown in Appendix B. Structural quantities, necessary for the magnetic calculations, are determined during the adatom deposition. These are the island labels i , the island volumes N_i , the number of atomic bonds between connected islands L_{ij} , and the average coordination numbers \bar{z}_i . If an adatom connects neighboring islands, it is randomly added to one of the islands.

2.2 Resulting nanostructured films

2.2.1 Different growth modes

In this subsection, we present resulting nanostructures, which demonstrate that different experimentally observed growth modes, such as the 3D-island or the layer-by-layer growth mode can be simulated by the appropriate choice of the layer-dependent parameters A_z .

Fig. 2.2 shows a snapshot resulting from a simulation of a 3D-island-type film with rectangular island shapes at coverage $\Theta = 1$ ML. In a first step, 250 island seeds are randomly distributed on a $4 \times 500 \times 500$ fcc-(001) unit cell with minimal mutual distances $r_{\min} = 26 r_o$, r_o being the interatomic distance, which considers the depletion range around the islands due to single-atom diffusion. Then, the growth scheme described in the previous section is applied, where we use the parameters $A_1 = 0.35$ eV $<$ $A_2 = 0.355$ eV $<$ $A_3 = 0.36$ eV $<$ $A_4 = 0.365$ eV, and the growth temperature $T_g = 300$ K. A very similar growth mode is found experimentally for Ni/Cu(001) films for coverages above 6 ML [150]. Fig. 2.3 shows a STM image of this system at 7.1 ML. On top of the sixth Ni layer randomly distributed 3D islands of few

⁵In reality, the formation of 3D islands often results from a nonequilibrium kinetic effect, where the hopping of an adatom over an island step edge onto the underlying layer is suppressed by an energy barrier (Ehrlich-Schwoebel barrier) [44, 149].

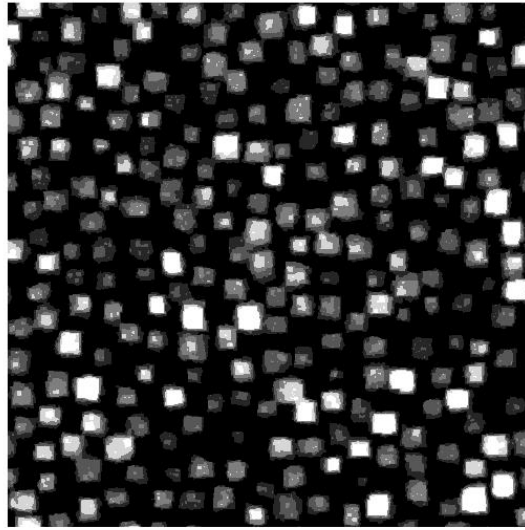


Figure 2.2: Simulation of a 3D-island growth mode with equilibrated island shapes at coverage $\Theta = 1.0$ ML. A $4 \times 500 \times 500$ unit cell with 250 islands is shown. Black represents the uncovered substrate, the different grey scales represent four adatom layers.

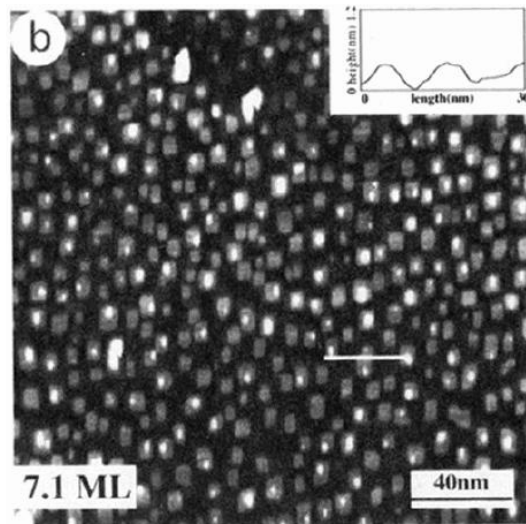


Figure 2.3: STM image of 7.1 ML Ni/Cu(001) showing 3D islands with rectangular shapes on top of the sixth Ni layer. The successive grey scales represent the different layers (darkest: 6th layer, brightest: 9th layer) (taken from Ref. [150]).

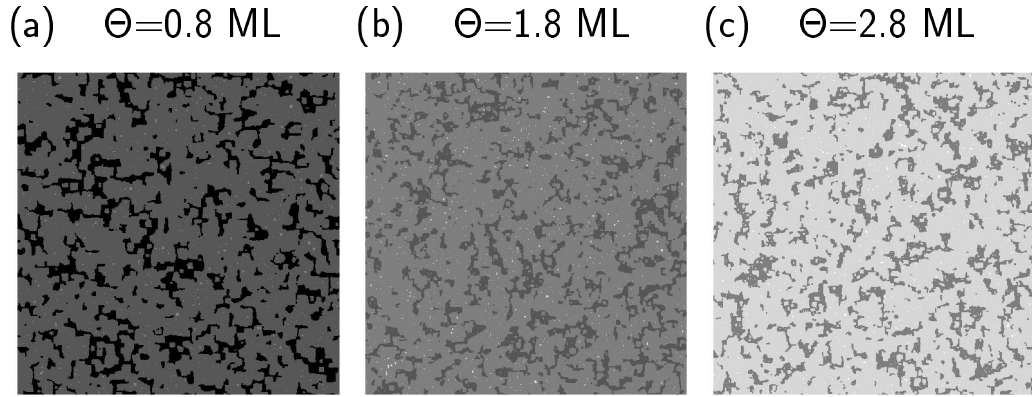


Figure 2.4: Simulation of a layer-by-layer growth mode, showing three different coverages. A particular layer starts to grow only after the preceding layer is almost completely filled. Black represents the uncovered substrate, the different grey scales represent four adatom layers. A $4 \times 500 \times 500$ unit cell is depicted.

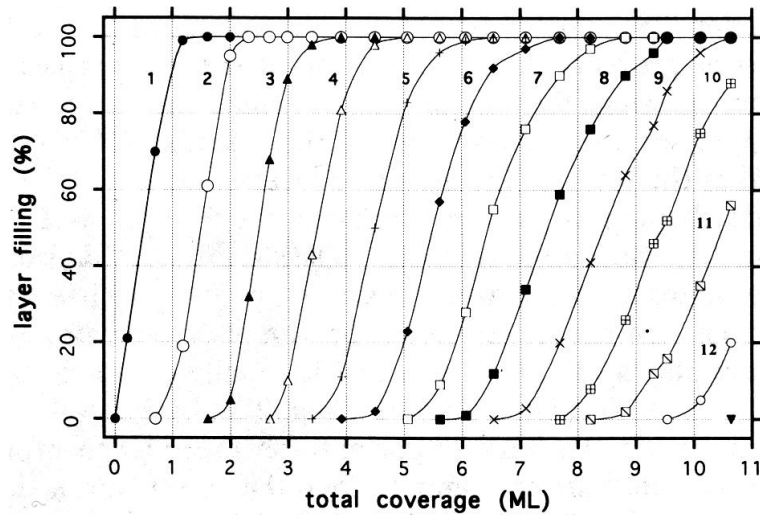


Figure 2.5: Experimental results for the layer filling as function of the film coverage of the Ni/Cu(001) system. In the coverage range up to ~ 3 ML an almost perfect layer-by-layer growth mode is observed (taken from Ref. [150]).

	A_1 [eV]	0.35
	A_2 [eV]	0.354
	T_g [K]	300
I	ρ_{is} [r_o^{-2}]	0.0025
I	r_{min} [r_o]	16
II	ρ_{is} [r_o^{-2}]	0.005
II	r_{min} [r_o]	10

Table 2.1: Growth parameters of the bilayer island growth mode. A_1 and A_2 are the layer-dependent effective binding parameters, T_g is the temperature during growth, ρ_{is} is the island density, and r_{min} is the minimal mutual distance of the island seeds in units of the interatomic distance r_o . In the present thesis, both versions I and II are applied.

layers height and with equilibrated island shapes are observed.

An example for the simulation of a layer-by-layer growth mode is presented in Fig. 2.4. In (a) the black substrate is almost completely covered, while few small islands already started to grow in the second adatom layer. In (b) and (c) the film coverage is increased by 1 ML each, showing the same behavior for the subsequent layers. For this, the binding parameters $A_1 = 0.40$ eV $>$ $A_2 = 0.39$ eV $>$ $A_3 = 0.38$ eV $>$ $A_4 = 0.37$ eV and the growth temperature $T_g = 300$ K are applied. An almost perfect layer-by-layer growth mode is experimentally observed again for Ni/Cu(001) ultrathin films [150], Fig. 2.5. In the coverage range up to ~ 3 ML, the subsequent layer starts to grow only after the preceding layer is almost completely filled.

2.2.2 Bilayer island growth

In this subsection, we present snapshots of a bilayer island growth mode which serves as a model system of the present study for the calculation of the magnetic properties.

Tab. 2.1 shows the parameters applied for this growth mode. First, the island seeds are randomly distributed in the first layer of a $2 \times 500 \times 500$ unit cell. In version I, the island density is adjusted to $\rho_{\text{is}} = 0.0025 r_o^{-2}$ (625 islands), the minimal mutual island distances amount to $r_{\text{min}} = 16 r_o$. In version II, the island density is doubled, resulting in $\rho_{\text{is}} = 0.005 r_o^{-2}$ and $r_{\text{min}} = 10 r_o$. Then, adatoms are deposited according to Eqs. (2.1) and (2.3) using the parameters $A_1 = 0.35$ eV $<$ $A_2 = 0.354$ eV, and $T_g = 300$ K.

In Fig. 2.6, we present snapshots of this growth mode (version I). For a better visualization, a small $2 \times 200 \times 200$ unit cell is depicted. In the initial stages of growth, (a), randomly located bilayer islands with almost rectangular shapes are present. With increasing film coverage, (b) and (c), the single

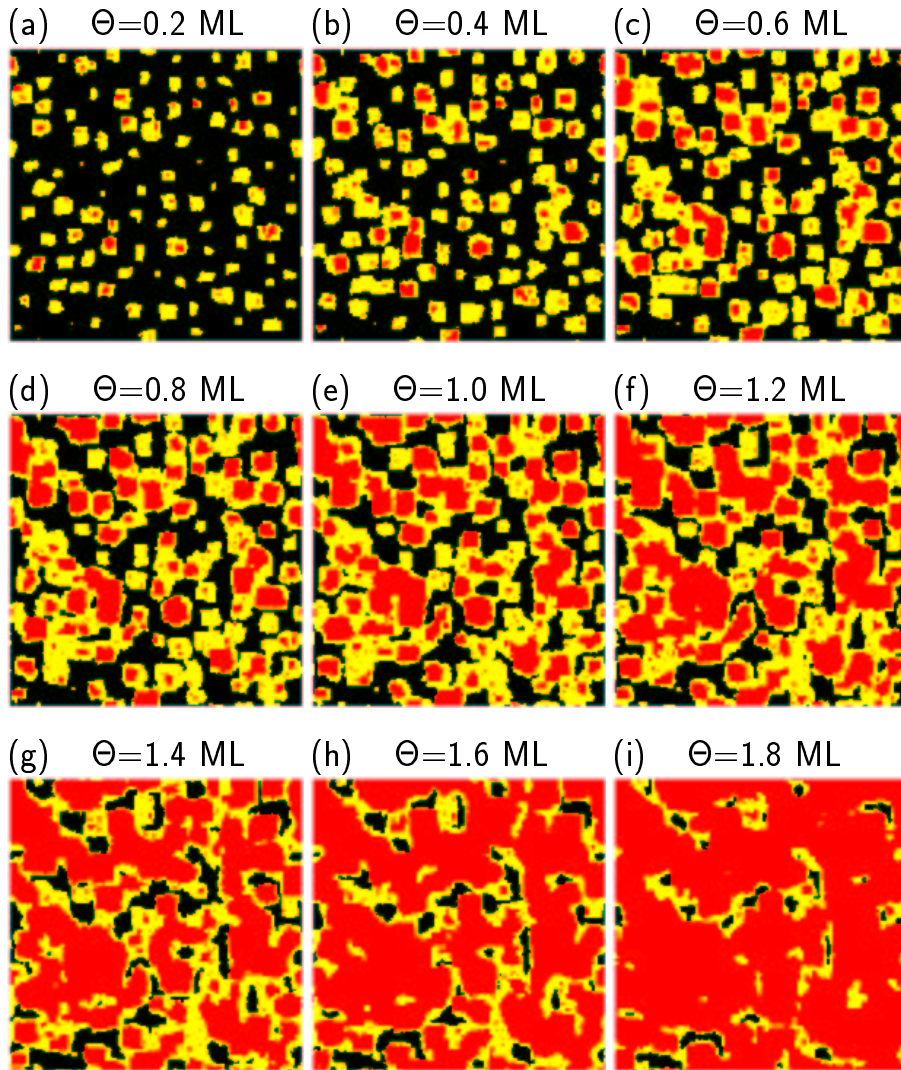


Figure 2.6: Results for the atomic structure of a thin film using a bilayer island-type growth mode. A $2 \times 200 \times 200$ unit cell with 100 islands is shown. Snapshots of several coverages Θ during growth are depicted. Black refers to the nonmagnetic substrate, light gray to the first and dark gray to the second magnetic layer.

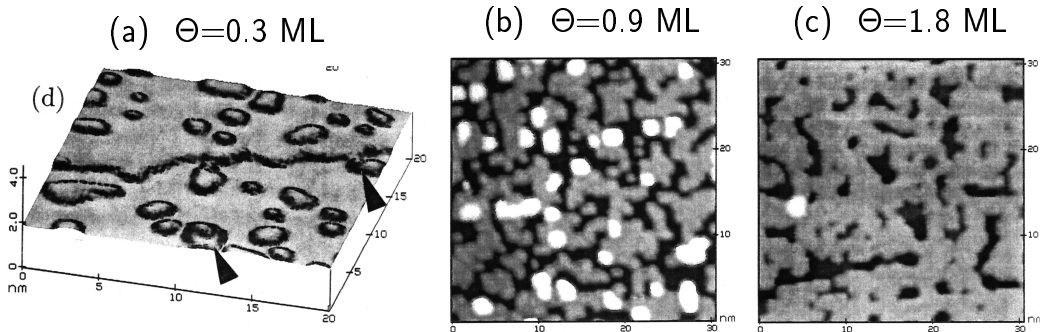


Figure 2.7: Initial bilayer growth mode of Co/Cu(001) as observed by STM. Three different coverages Θ are depicted: (a) 0.3 ML, the arrows indicate islands with second layers, (b) 0.9 ML, black refers to the substrate, grey to the 1st and white to the 2nd adatom layer, (c) 1.8 ML, black refers to the 1st, grey to the 2nd and white to the 3rd adatom layer (taken from Ref. [144]).

islands start to coagulate and form island clusters, which are still finite. By inspection, one observes that percolation of the islands to a connected structure evolves between $\Theta = 0.8$, (d), and 1.0 ML, (e). A more precise analysis of the percolation coverage Θ_P is given in the next subsection. Continued film growth, (f) - (i), leads to a connected thin film. In this coverage range, the system still exhibits a distinct irregular nanostructure. Isolated islands and island clusters vanish rapidly upon further adatom deposition. The coverage $\Theta = 2.0$ ML corresponds to a smooth magnetic film with two closed layers (not shown). The resulting static atomic structure is similar to the one observed experimentally for the Co/Cu(001) system, see Fig. 2.7 and Fig.1.1, p. 15.

In Fig. 2.8, probability distributions of the structural quantities of the bilayer island growth mode (version II), which serve as input for the magnetic calculations, are depicted. Distributions for different film coverages Θ are shown for the island size N_i , the number of atomic bonds between connected islands L_{ij} , and the number of next neighbored islands to which the islands are connected.

2.2.3 Percolation threshold

In this subsection, we determine the critical coverage Θ_P for two-dimensional percolation of the bilayer island growth mode. Θ_P has an important impact on the magnetic properties of a growing island-type film. If we assume exclusively *short-range* nearest-neighbor magnetic interactions between magnetic moments, then the existence of a percolated (infinite) cluster of nearest-neighbor moments is a *prerequisite* for long-range magnetic ordering.

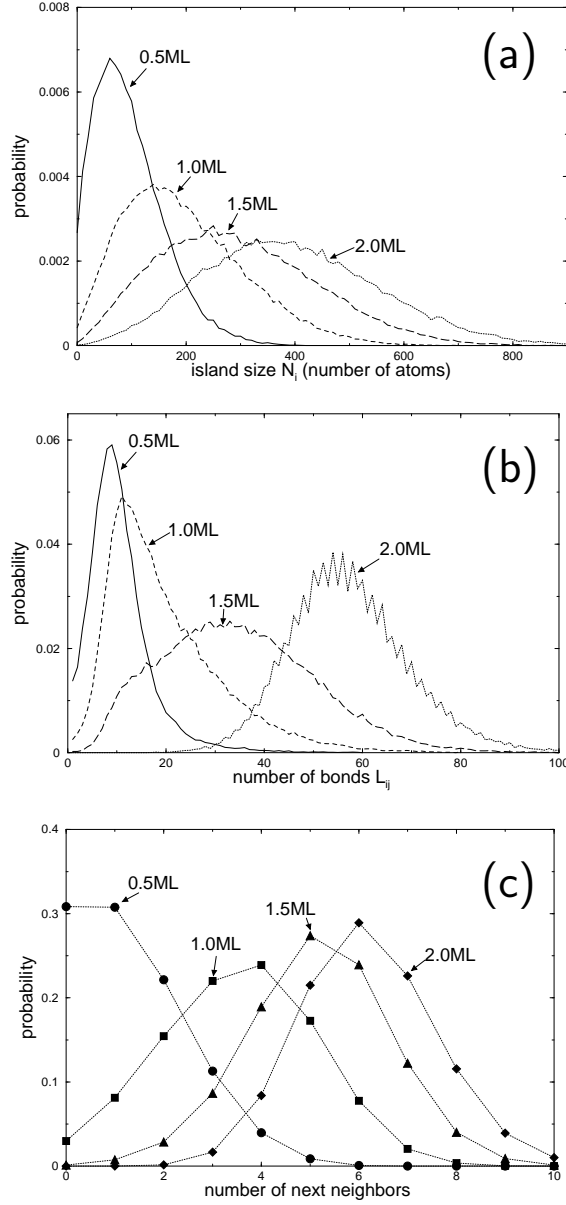


Figure 2.8: Probability distributions of structural quantities, used as input for magnetic calculations, for different coverages Θ of the bilayer island growth mode (version II). Distributions are shown for the island size N_i , the number of atomic bonds between connected islands L_{ij} , and the number of next neighbored islands to which the islands are connected.

Usually, for the so-called ‘site percolation’ problem, sites of an empty lattice are *randomly* occupied with concentration (probability) $c \in [0, 1]$.⁶ For an *infinite* lattice, the probability $R_\infty(c)$ of finding a percolating cluster (infinite cluster of nearest-neighbored occupied sites) becomes zero for $c < c_P$ and unity for $c \geq c_P$. At the percolation threshold c_P , the system undergoes a geometric phase transition [156]. The order parameter of this percolation phase transition is defined by the ‘percolation probability’ $P_\infty(c)$ (also called the ‘strength of the network’), given by the fraction of occupied sites which belong to the percolating cluster. The percolation probability behaves roughly like⁷

$$P_\infty(c < c_P) = 0 \quad , \quad P_\infty(c \geq c_P) > 0 \quad . \quad (2.4)$$

For *finite* $L \times L$ lattices, the percolation probability $P_L(c)$ can be calculated by usage of the fraction

$$P_L(c) = \frac{C_{\max}(c)}{N_{\text{occ}}(c)} \quad , \quad (2.5)$$

where C_{\max} is the number of sites of the largest cluster and N_{occ} is the total number of occupied sites. The average of $P_L(c)$ over different structural realizations of the percolation problem approximates $P_\infty(c)$ [156].

Generally, percolation thresholds c_P depend on the type of the lattice and the spatial dimension, and can be calculated analytically only for few cases. Most of the time numerical estimations are unavoidable, e. g. for the square lattice $c_P \approx 0.59$ was obtained [177]. Clearly, in the case of growing thin films, the percolation threshold Θ_P is *not* given by the concentration c_P , since in the first case the adatom deposition does not evolve randomly. Rather, the percolation *coverage* Θ_P depends sensitively on the growth mode of the film, the island shapes, etc.

In the following, we determine the percolation coverage Θ_P of the bilayer model system numerically, using Eq. (2.5). The quantity $C_{\max}(\Theta)$ is calculated by use of the Hoshen-Kopelman algorithm [68], see Appendix C.

Fig. 2.9 shows the percolation probability $P_L(\Theta)$ of the first adatom layer as function of the film coverage Θ . Results for different lattice sizes L are depicted. Each curve is obtained by averaging over at least 20 different realizations of the bilayer growth mode (version I). For $L = 1000$ the error bars indicate the statistical error resulting from the averaging procedure. As usually obtained for finite systems, $P_L(\Theta)$ rises smoothly for coverages below

⁶The percolation problem can be found in completely different types of research fields and is therefore of major interest. Examples are the spread of a forest fire, the propagation of rumors or electrical conductance in a mixture [156].

⁷For dimensions $d > 1$, a critical behavior of second order according to $P_\infty \propto (c - c_P)^\beta$, $c \geq c_P$ is expected, analogously to a thermal phase transition at critical temperature T_c .

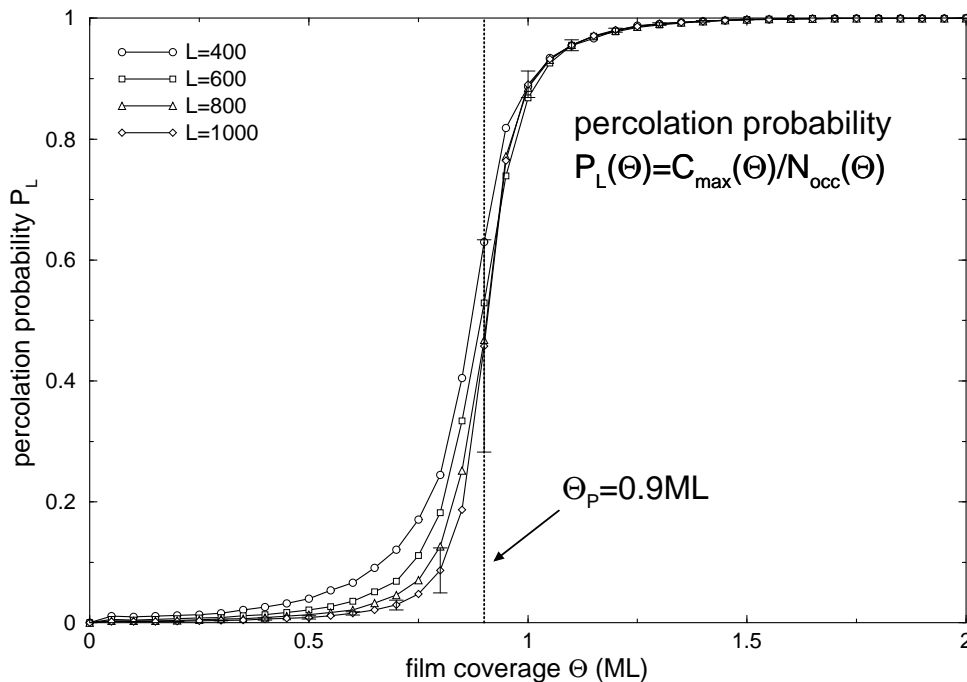


Figure 2.9: The percolation probability $P_L(\Theta)$ of the first adatom layer as function of the film coverage Θ for the bilayer island growth mode (version I). Curves for different lattice sizes L are shown. For $L \rightarrow \infty$ we choose the percolation threshold $\Theta_P = 0.9 \pm 0.05$ ML.

Θ_P rather than showing the singular behavior described by Eq. (2.4). For increasing lattice size L , this finite size effect becomes smaller and the curves become steeper. For $L \rightarrow \infty$, we extrapolate the percolation to happen at the film coverage $\Theta_P = 0.9 \pm 0.05$ ML.⁸ A doubling of the island density (version II of the model system) revealed approximately the same value.

In the remainder of this section, we discuss experimental results for the percolation coverage Θ_P^{exp} of Co/Cu(001) ultrathin films. Schumann *et al.* were the first who attributed the onset of room-temperature long-range ferromagnetism of Co/Cu(001) at a critical coverage to a percolation phase transition [148]. Near the critical coverage, they found a power-law dependence of the magnetic susceptibility with the same critical exponent as obtained from renormalization-group calculations of the randomly diluted Ising model on a square lattice [74]. Bovensiepen *et al.* identified the percolation to happen at $\Theta_P^{\text{exp}} = 1.7$ ML, where they observed a discontinuous ‘jump’ of the Curie temperature of the long-range ferromagnetic order [17, 133]. The percolation of the magnetic Co film is assumed to happen in the second layer due to

⁸We do not perform a finite size scaling analysis, since the exact value of Θ_P for an infinite system is not needed for our purposes.

intermixing of Co adatoms with Cu substrate atoms, which is observed for early stages of film growth [48, 114, 125].

In principle, an intermixing of adatoms and substrate atoms could be included in our simple growth model, leading to a percolation of the adatom film in the second layer. The main reason for the neglect of intermixing in the present study is that there is only incomplete knowledge of the positions of the Cu and Co atoms in the entire growth range up to ~ 2 ML; the coverage-dependent morphology of the magnetic Co film (Co island sizes, shapes, and positions) remains unclear. Thus, in the present thesis the bilayer island growth mode serves as the model system for magnetic calculations.

